

Article

A Two-Grid Interline Dynamic Voltage Restorer Based on Two Three-Phase Input Matrix Converters

Sergio Constantino Yáñez-Campos ^{1,2,*}, Gustavo Cerda-Villafaña ² and José Merced Lozano-García ² 

¹ National Technological of Mexico, Coordination of Electronic Engineering, Higher Technological Institute of Irapuato, Irapuato 36820, Mexico

² Department of Electronic Engineering, DICIS, University of Guanajuato, Salamanca 36787, Mexico; gcerdav@ugto.mx (G.C.-V.); jm.lozano@ugto.mx (J.M.L.-G.)

* Correspondence: sergioc.yanezc@gmail.com; Tel.: +521-462-158-2381

Abstract: Energy quality problems can cause diverse failures of sensitive equipment. Dynamic voltage restorers (DVRs) are devices that have been proposed to protect sensitive loads from voltage sag effects. However, the compensation capacity of DVRs is limited by the amount of energy stored in the restorer. One way to overcome this limitation is to use the interline DVR (IDVR) structure in which two or more DVRs connected to different feeders share a common DC-link. This paper proposes a new IDVR topology based on two three-phase input matrix converters (TTI-MC) without a capacitor in the dc-link. The TTI-MC integrates the power from two feeders and synthesizes the dc-link voltage. The inverters take the dc-link voltage and generate the appropriate compensation voltages to keep the load voltages stable. Each one of the inverters has its own modulation algorithm which are synchronized with the TTI-MC control. Inverter control is carried out in the reference frame dq and a modified space vector pulse width modulation (MSV-PWM) technique is used. TTI-MC control is performed in the dq reference frame with proportional-integral controllers and the modulation is based on the carrier-based pulse width modulation (MCB-PWM) technique. The proposed Two Input Interline DVR (TI-IDVR) extends its compensation range and has multifunctional capabilities. The efficiency of the proposed TI-IDVR is corroborated by simulations on MATLAB/Simulink.

Keywords: carrier-based pulse width modulation (MCB-PWM); interline dynamic voltage restorer (IDVR); matrix converters (MC); power quality (PQ); space vector modulation (SVM)



Citation: Yáñez-Campos, S.C.; Cerda-Villafaña, G.; Lozano-García, J.M. A Two-Grid Interline Dynamic Voltage Restorer Based on Two Three-Phase Input Matrix Converters. *Appl. Sci.* **2021**, *11*, 561. <https://doi.org/10.3390/app11020561>

Received: 29 October 2020

Accepted: 6 December 2020

Published: 8 January 2021

Publisher's Note: MDPI stays neutral with regard to jurisdictional claims in published maps and institutional affiliations.



Copyright: © 2021 by the authors. Licensee MDPI, Basel, Switzerland. This article is an open access article distributed under the terms and conditions of the Creative Commons Attribution (CC BY) license (<https://creativecommons.org/licenses/by/4.0/>).

1. Introduction

Power quality (PQ) problems have been extensively investigated in recent years. This is because poor PQ causes failures or malfunctions in loads sensitive to voltage variations. Therefore, voltage quality is considered the most common and important parameter for end users. Although there are a variety of problems that can cause poor PQ, voltage sags have become one of the most important problems due to the increase in use of equipment that are sensitive to voltage variations [1–3].

In an effort to mitigate or eliminate the adverse effects caused by voltage variations in sensitive equipment, devices based on power electronics called custom power devices (CPD) [4–6] have been developed. Among these devices, dynamic voltage restorers (DVRs) stand out due to their operational advantages.

DVRs are an economical solution and are technically the most suitable device to protect sensitive loads from voltage sags. Normally, a DVR is installed where the distribution grid feeds large industrial plants or many sensitive loads. The operation principle of the DVR is to inject an appropriate voltage in series with the power supply through an injection transformer to restore the supply voltage under abnormal conditions. The magnitude and phase angle of the injected voltage is variable; therefore, an active and reactive power exchange is generated between the DVR and the distribution system or the load.

Due to the importance of DVRs in the mitigation of disturbances in electrical grids, different topologies and control strategies have been developed to improve their performance [7–10]. The compensation range of DVRs has also been extended to provide multi-functional capabilities [11,12]. Other studies include the use of Matrix Converter (MC) in the topology of DVR [12–14].

While DVRs are widely used in mitigating voltage disturbances, their ability to compensate for long-term and deep voltage sags is limited due to the amount of energy stored in the same DVR structure. To overcome this limitation, a type of DVR called an interline DVR (IDVR) [15–25] has been developed.

The IDVR is a system that consists of several DVRs that protect sensitive loads on different feeders in the distribution grid and share a common dc-link (Figure 1). When one of the DVRs of the IDVR system compensates for a voltage sag, it takes energy from the dc-link. At the same time, the other DVRs fill the energy dc-link to keep its voltage at a specific level. An example of a potential application of this scheme is in a custom power park (CPP) [26–30] where power is provided by multi-feeders (i.e., different power supplies connected to different network transformers); in this way, they are electrically separated. Sensitive loads in these parks can be protected by DVRs connected respectively to their load. The dc-links of these DVRs can be connected to a common terminal, thus forming the IDVR system. This can reduce the cost of the energy storage system. Sharing a common dc-link substantially reduces the size energy storage device of the dc-link compared to a system in which loads are protected by independent DVRs with separate energy storage systems.

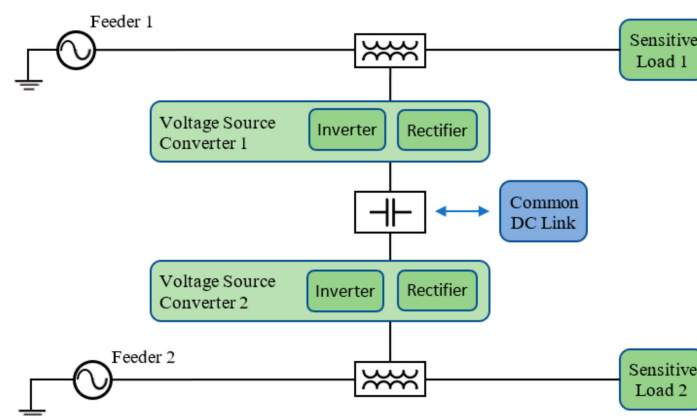


Figure 1. Schematic diagram of the interline dynamic voltage restorers (IDVRs) proposed in the literature. Where DC is Direct Current.

The IDVR provides a way to dynamically replenish the energy available in the energy storage device of the dc-link. However, the compensation capacity of the IDVR depends largely on the load power factor [17–20].

With the aim of extending the compensation range of the IDVR in the event of deep and long-term voltage sags and also of improving its performance in loads with a high power factor, this paper presents a new IDVR topology based on two three-phase input matrix converters (TTI-MC), hence referred to as the two input IDVR (TI-IDVR).

In [12], we present a two-input DVR based on the TTI-MC to be applied in CPPs with similar characteristics to those mentioned above. In this paper, features are added to the TI-IDVR that allow a more efficient use of the power provided by the feeders. The proposed TI-IDVR integrates the power of the two feeders to compensate for the disturbances that occur in either of the two feeders.

An important contribution of the proposed TI-IDVR with respect to other IDVRs consists of the following: if a swell occurs in any of the feeders, the TI-IDVR takes excess power from the feeder that presents the fault to compensate for the disturbance and does not take power from the healthy feeder; that is, in the case of a swell, the proposed TI-IDVR

behaves like a conventional DVR, unlike other IDVRs that take power from the healthy feeder to compensate for the swell in the feeder that has the fault.

The use of an IDVR in multi-feeder distribution systems to mitigate PQ problems has been presented in several publications. In [16,17,19,21], an IDVR is used to mitigate sags. In [15], an IDVR is used to compensate for balanced and unbalanced sags. The compensation of sags, swells and voltage imbalance using an IDVR is presented in [18]. In [22,23], an IDVR is used to mitigate sags and swells. On the other hand, it should be mentioned due to the importance of DVRs within the IDVR shown in Figure 1, design strategies have been presented that take into consideration that the IDVR must be able to compensate for different types of voltage disturbances in each one of the feeders and the minimum DVR voltage ratings are selected in terms of the generation of the compensation voltage and the energy injection to the capacitor in the dc-link [24,25].

The proposed TI-IDVR is able to compensate for balanced and unbalanced sags and swells, as well as voltage distortion. Additionally, the TI-IDVR can also compensate for deep and long-term voltage sags and voltage interruptions. That is, the TI-IDVR has multi-functional capabilities.

In this sense, an important contribution of this work is that, when a voltage interruption occurs in one of the feeders, the proposed TI-IDVR behaves as a reconfiguration and compensation device in multi-feeder distribution systems or in a CPP. All of these features differentiate it from other IDVRs that, as mentioned above, are aimed at compensating sags and swells in one of the feeders.

The control algorithm is carried out in the reference frame dq and can be divided into two parts that are synchronized with each other: (a) the control of the current source inverters (CSIs), and (b) the control of the TTI-MC. There are two feeders in the TI-IDVR system, each with its respective load. The system starts with the voltage measured in feeder 1 (or 2), which is compared with the nominal voltage of sensitive load 1 (or 2) to obtain the difference between them, and thus compensate for the disturbances in feeder 1 (or 2). The injected voltage is synthesized by the respective CSI using the space vector modulation (SVM) scheme. For this, the control algorithm requires the phase angle information of the load voltage in the reference frame dq . The TTI-MC integrates the voltages of the two feeders to build the voltage in the virtual dc-link; this is done by implementing the carrier-based pulse width modulation (MCB-PWM) scheme with two references. The control algorithm generates two sets of reference signals (one set for each of the feeders). The control is carried out in the reference frame dq to obtain a unit power factor in both feeders, and also in their corresponding loads.

In this article, we propose a new IDVR topology based on the TTI-MC that can be used in multi-feeder systems or in a CPP. The relevance of the proposed TI-IDVR is based on the following points: (1) the proposed TI-IDVR has two three-phase inputs; in this way, it integrates the power taken from the two feeders, unlike other IDVRs; (2) the proposed TI-IDVR is able to mitigate different types of PQ problems (that is, it has a multi-functional capacity in the mitigation of disturbances); (3) the TI-IDVR has the ability to behave as a reconfiguration and compensation device in multi-feeder distribution systems and in CPPs; (4) the proposed TI-IDVR consumes power from the feeders depending on the type of disturbance that arises. For example, if a sag arises, the TTI-MC draws power from the two feeders to build the voltage on the dc-link. If the disturbance is a swell, the TTI-MC only draws power from the failed feeder. In contrast, the IDVRs proposed in the literature draw power from the healthy feeder to fulfill the needs of the energy storage device in the dc-link regardless of whether the disturbance is a sag or a swell. In this sense, the proposed TI-IDVR makes a more efficient use of the power provided by the feeders; (5) it does not use external energy storage systems; (6) it has no elements for energy storage in the dc-link, therefore, it is not necessary to control its voltage. Energy storage systems, such as capacitors, have played an important role in power electronic converters, specifically in AC-DC-AC converters. However, capacitors have been shown to be the components that most frequently fail in power electronic systems [31–33]. To overcome this

drawback, a TI-IDVR based on the TTI-MC without a capacitor in the dc-link is proposed as a good alternative; (7) the compensation range against deep and long-term voltage sags is extended. The performance of the proposed TI-IDVR was verified by simulating different types of disturbances. The simulations were carried out in the MATLAB/Simulink environment.

The arrangement of this work is as follows: the operation principle of the proposed TI-IDVR is discussed in Section 2. Section 3 presents the mathematical analysis that describes the TI-IDVR operation in the presence of voltage sags and swells. The modulation schemes of the CSIs and the TTI-MC are addressed in Sections 4 and 5, respectively. The control objectives of the proposed TI-IDVR and the control algorithms of the CSIs and the TTI-MC are analyzed in Section 6. The results of the simulation of the TI-IDVR are discussed in Section 7. Finally, the conclusions of this work are presented in Section 8.

2. Operation of the TI-IDVR

The IDVR system consists of several DVRs connected by different feeders, which share a common dc-link. The proposed TI-IDVR system shown in Figure 2 employs two DVRs connected to two different feeders originating from two network substations. These two feeders can have the same voltage level or have different voltage levels. The system consists of two independent feeders, a sensitive load on each feeder, a TTI-MC, two CSIs to synthesize the voltage to be injected into the grid, two injection transformers, two input filters and two output filters.

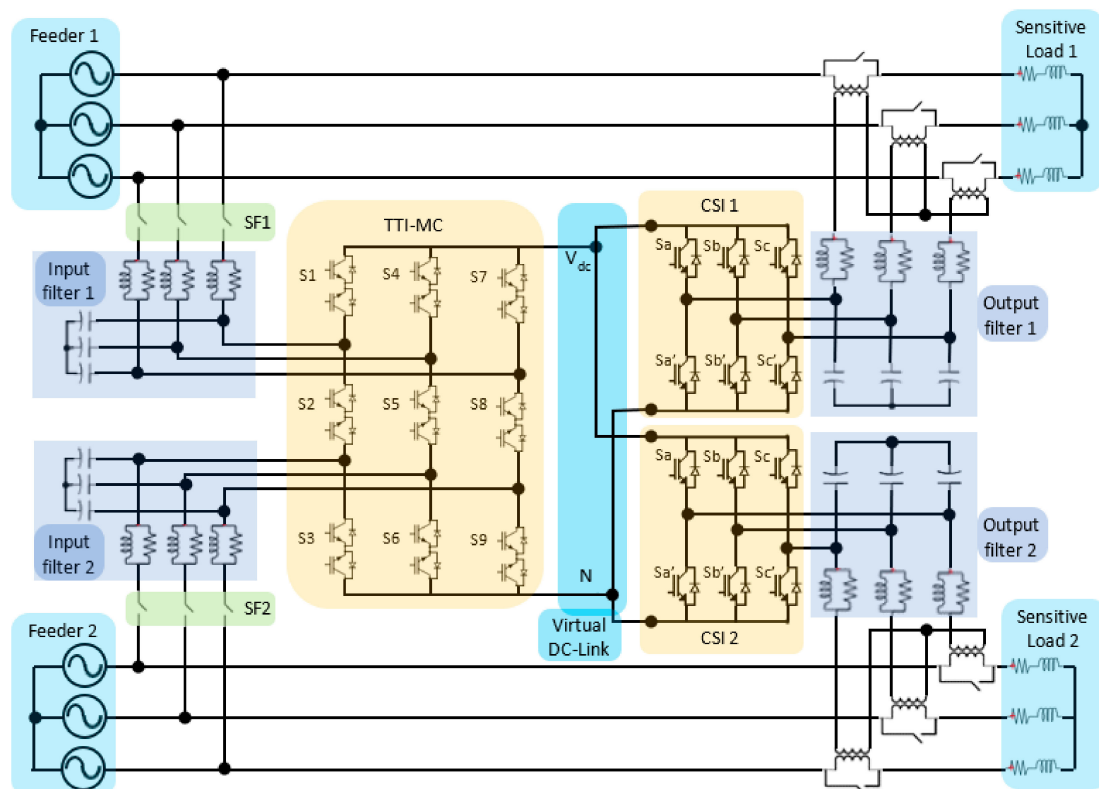


Figure 2. Schematic diagram of the proposed two input interline dynamic voltage regulator (TI-IDVR). CSI: current source inverter; TTI-MC: two three-phase input matrix converter. Where, SF are the switches that connect and disconnect the feeders and S_n are the switching elements of the TTI-MC and the CSIs, with $n = 1, 2 \dots$ and $n = a, b, c$, respectively.

As shown in Figure 2, the proposed TI-IDVR presents the configuration of two DVRs (without energy storage systems) connected on the source side without a capacitor on the dc-link. The merge of the two DVRs is done by replacing the two shunt converters of the DVRs with a TTI-MC. In this way, the considerations related to this topology are taken [7]:

(a) when a voltage sag occurs, the shunt converter takes the remaining voltage and current from the feeder to maintain the full load power at nominal voltage; (b) a saving is obtained in the energy storage system; (c) there is the capacity to compensate for long-term voltage sags; (d) it is recommended that the feeders be robust since these topologies draw more current from the line during the fault. In this sense, even if the feeders are robust and capable of providing high currents, in practice, the available current could be limited by the overcurrent protection devices in the distribution line transformers; and (e) a saving is obtained by not using energy storage devices on the dc-link.

It should be mentioned that although the use of TTI-MCs has not been widely adopted in IDVR topologies, it provides the benefit of expanding the compensation range by integrating the two feeders to power the TI-IDVR's virtual dc-link.

Functionally, depending on the type of disturbance to compensate for, the proposed TI-IDVR can perform as a conventional DVR or as an IDVR. When a voltage swell appears in one of the feeders, the TI-IDVR behaves like a DVR and draws excess power from the failed feeder to compensate for the disturbance and keep the load voltage at its nominal value. In this way, the TI-IDVR does not draw power from the healthy feeder to compensate for the voltage swell in the faulty feeder. On the other hand, when the disturbance is a voltage sag, the TI-IDVR behaves like an IDVR and draws power from the two feeders to compensate for the disturbance and to keep the voltage on the load at its nominal value. In this case, the TI-IDVR integrates the power from the two feeders and is therefore capable of compensating for deep and long-term voltage sags.

In terms of the modes of operation of the converters, when a disturbance occurs in one of the feeders, the series converter (CSI) corresponding to the failed feeder operates in compensation mode and mitigates the disturbance. At the same time, the shunt converter (TTI-MC) operates in power flow control mode. If the disturbance is a voltage swell, the TTI-MC transfers the excess power from the faulty feeder to the virtual dc-link. If the disturbance is a voltage sag, the TTI-MC integrates the power from the two feeders and transfers it to the virtual dc-link. The CSI that is operating in compensation mode takes power from the virtual dc-link and builds the compensation voltage to mitigate the disturbance in the faulty feeder.

On the other hand, since the two feeders of the TI-IDVR system in Figure 2 are connected to two different grid substations, it is reasonable to suppose that a disturbance in one of the feeders would have a negligible impact on the other feeder [17]. In this way, the two feeders in the system can be considered as two independent sources. Therefore, the proposed TI-IDVR has a permanent power supply; therefore, compensation for deep and long-term voltage sags and also voltage interruptions can be guaranteed.

3. TI-IDVR System Analysis

For the analysis of the proposed TI-IDVR shown in Figure 2, we assume ideal conditions and that the feeders and loads have the same nominal characteristics. It is also considered that a voltage sag arises in feeder 1. Under these considerations, it is assumed that the series converter (CSI 1) operates in compensation mode and the shunt converter (TTI-MC) operates in power flow control mode. Figure 3a shows the relationship of the voltage vectors or voltage phasors in this case. Taking into consideration Figures 2 and 3a, the following equation can be written:

$$\vec{V}_{L1, rated} = \vec{V}_{F1, sag} + \vec{V}_{comp, sag} \quad (1)$$

where, $\vec{V}_{L1, rated}$, $\vec{V}_{F1, sag}$ and $\vec{V}_{comp, sag}$ are the voltage vectors of load voltage 1, feeder 1 voltage (with sag), and compensation voltage injected by the TI-IDVR, respectively.

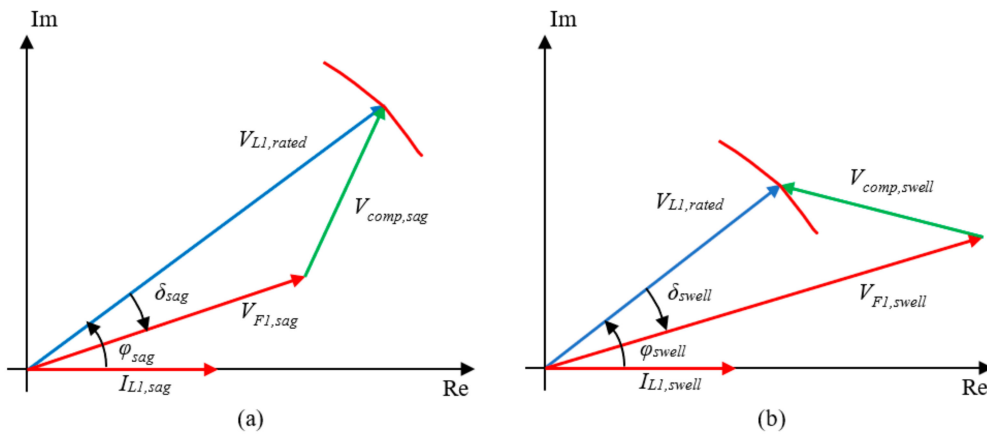


Figure 3. Phasor diagram of feeder 1 voltage, the load 1 voltage, and compensation voltage. (a) Voltage sag and (b) voltage swell. Where, $\vec{V}_{L1,rated}$, $\vec{V}_{F1,sag}$, $\vec{V}_{comp,sag}$, $\vec{V}_{F1,swell}$ and $\vec{V}_{comp,swell}$ are the voltage vectors of load voltage 1, feeder 1 voltage (with sag), sag compensation voltage injected, feeder 1 voltage (with swell) and swell compensation voltage injected. $\vec{I}_{L1,sag}$ and $\vec{I}_{L1,swell}$ are the vectors of the load currents in the presence of sag and swell respectively. δ_{sag} and ϕ_{sag} are the angles between the vector $\vec{V}_{L1,rated}$ and the vectors $\vec{V}_{F1,sag}$ and $\vec{I}_{L1,sag}$ respectively. In the same way, δ_{swell} and ϕ_{swell} are the angles between the vector $\vec{V}_{L1,rated}$ and the vectors $\vec{V}_{F1,swell}$ and $\vec{I}_{L1,swell}$.

On the other hand, neglecting the voltage drop in the CSI output filter and the injection transformer, the absolute value of the compensation voltage $|\vec{V}_{comp,sag}|$ is related to the voltage in the virtual dc-link (V_{dc}), the modulation index of the CSI (M), and the transformation ratio of the injection transformer (a , ratio of the converter side to the network side) in the following way:

$$|\vec{V}_{comp,sag}| = aMV_{dc} \tag{2}$$

The per unit value of the voltage sag ($V_{sag,pu}$) based on the load voltage nominal value ($V_{base} = |V_{L1,rated}|$) is defined as follows:

$$V_{sag,pu} = \frac{|V_{L1,rated}| - |V_{F1,sag}|}{|V_{L1,rated}|} \quad V_{sag,pu} = 1 - |V_{F1,sag,pu}| \tag{3}$$

Now, for clarity, assuming that the voltages $\vec{V}_{L1,rated}$ and $\vec{V}_{F1,sag}$ are in phase, Equation (1) can be written as follows:

$$|V_{L1,rated}| = |V_{F1,sag}| + |V_{comp,sag}| \tag{4}$$

The purpose of the TI-IDVR is to maintain the load voltage at its nominal value ($|V_{L1}| = |V_{L1,rated}|$), in this way, using Equation (4), it can be written as:

$$1 = |V_{F1,sag,pu}| + |V_{comp,sag,pu}| \tag{5}$$

Combining Equations (2), (3) and (5) we can write:

$$V_{sag,pu} = aMV_{dc,pu} \tag{6}$$

The maximum value of a voltage sag that can be compensated by the CSI1 of the TI-IDVR can be obtained considering that the maximum value of the modulation index in Equation (6) is 1 ($M = 1$). In this way, we can write:

$$V_{sagmax,pu} = aV_{dc,pu} \tag{7}$$

This equation indicates that the maximum value of a voltage sag ($V_{sagmax,pu}$) that can be fully compensated by a conventional DVR is directly related to the voltage present on the dc-link and to the transformation ratio of the injection transformer. Theoretically, Equation (7) states that a conventional DVR can cope with any voltage sag value. However, there are some inherent limitations to the DVR configuration or topology. For a DVR with topology but without a power storage system connected on the feeder side (in this case feeder 1) and without a capacitor on the dc-link, the voltage on the dc-link can be estimated by $V_{dc,pu} = |V_{F1,pu}|$; then, Equation (7) can be written as:

$$V_{sagmax,pu} = a|V_{F1,pu}| \tag{8}$$

This equation indicates that for a DVR in this topology, the maximum value of a voltage sag that can be fully compensated by the DVR is limited by the voltage present in the voltage supply. That is, if we suppose that $a = 1$, Equation (8) tells us that the DVR under this configuration can compensate for, at most, a voltage sag of 0.5 pu.

On the other hand, the proposed TI-IDVR is formed by the merge of two DVRs without energy storage systems connected on the side of the power supply and without a capacitor in the dc-link. The merge of the two DVRs is done by replacing the shunt converters of both DVRs for the TTI-MC as shown in Figure 2. Taking the reasoning used to obtain Equation (2), we can say that the voltage on the dc-link (V_{dc}) is directly related to the voltages of the two feeders through the TTI-MC. Now, neglecting the voltage drop across the TTI-MC input filters, the voltage value on the dc-link relates to the feeder voltages (V_{F1} y V_{F2}) and the modulation index of the TTI-MC (M_{TTI-MC}) as follows:

$$\begin{aligned} V_{dc} &= M_{TTI-MC}(|V_{F1}| + |V_{F2}|) \\ V_{dc,pu} &= M_{TTI-MC}(|V_{F1,pu}| + |V_{F2,pu}|) \end{aligned} \tag{9}$$

The maximum voltage value on the virtual dc-link (V_{dcmax}) that the TTI-MC can provide can be obtained by considering that the maximum value of the TTI-MC modulation index in Equation (9) is 1 ($M_{TTI-MC} = 1$). In this way, we can write:

$$V_{dcmax,pu} = |V_{F1,pu}| + |V_{F2,pu}| \tag{10}$$

This equation indicates that in the absence of disturbances, the maximum voltage value on the virtual dc-link can be equal to 2 pu, $V_{dcmax,pu} = 2$ pu, and in the presence of a voltage sag in feeder 1, $V_{dcmax,pu} > 1$ pu.

If $V_{dcmax,pu} = V_{dc,pu}$ in Equation (7) we obtain the following expression:

$$V_{sagmax,pu} = aV_{dcmax,pu} \tag{11}$$

This equation indicates that for the proposed TI-IDVR, the maximum value of a voltage sag that can be fully compensated for in feeder 1 by the TI-IDVR is limited by the maximum voltage present on the virtual dc-link. Now, assuming a unit conversion ratio in the injection transformer ($a = 1$) and substituting Equation (10) into Equation (11), we obtain:

$$V_{sagmax,pu} = |V_{F1,pu}| + |V_{F2,pu}| \tag{12}$$

Considering ideal conditions and that $V_{F1,rated} = V_{F2,rated}$, this expression clearly shows that the maximum value of a voltage sag that can be fully compensated in feeder 1 by the TI-IDVR depends directly on the sum of the voltages of the two feeders. Theoretically, Equation (12) indicates an increase in the compensation range. Therefore, the proposed TI-IDVR has the ability to compensate for voltage sags greater than 0.5 pu. For example, suppose an extreme case where feeder 1 suffers a voltage interruption and the voltages on the feeders are $V_{F1Int,pu} = 0.05$ pu and $V_{F2,pu} = 1$ pu. Now, substituting the values of the voltages in pu of the feeders in Equation (12), we have $V_{sagmax,pu} = 1.05$ pu. Theoretically this value is outside the range of a voltage interruption. Therefore, the voltage interruption

in feeder 1 can be compensated for by the CSI1 of the TI-IDVR. It should be noted that for this configuration of the DVRs, it is assumed that the power supplies are strong or robust enough to withstand a higher current demand when compensating for voltage sags.

Now, suppose the value of the feeders is different and $|V_{F1, rated}| > |V_{F2, rated}|$. If we consider that a sag appears in feeder 2, Equation (12) can be written as follows:

$$V_{F2, sagmax} = |V_{F1, rated}| + |V_{F2, sag}| \tag{13}$$

This expression tells us that a sag of any magnitude that occurs in feeder 2 can be compensated for, including voltage interruption. This is because $|V_{F1, rated}| > |V_{F2, rated}|$.

On the other hand, if the sag appears in feeder 1, the magnitude of feeder 2 imposes limits on the value of the sag to compensate. Considering Figures 2 and 3a it can be written as:

$$|V_{L1, rated}| = |2V_{F1, sag}| + |V_{F2, rated}| \tag{14}$$

$$|2V_{F1, sag}| = |V_{L1, rated}| - |V_{F2, rated}| \tag{15}$$

since $|V_{F1, rated}| > |V_{F2, rated}|$, we can write:

$$|V_{L1, rated}| = k|V_{F2, rated}|; \quad k > 1 \tag{16}$$

where k can be defined as the relationship between the feeders. Thus, Equation (15) can be written as:

$$|2V_{F1, sag}| = k|V_{F2, rated}| - |V_{F2, rated}| \tag{17}$$

$|V_{F1, sag}| = |S'V_{F1, rated}|$, where S is the sag value that by definition has values between 0.9 and 0.1. In this way, we define $S' = (1-S)$. Substituting in Equation (17), we have:

$$|2S'V_{F1, rated}| = |V_{F2, rated}|(k - 1) \tag{18}$$

Combining Equations (16) and (18) gives us:

$$|2S'kV_{F2, rated}| = |V_{F2, rated}|(k - 1) \tag{19}$$

considering that $S' = (1-S)$ and solving for S:

$$S = \frac{1 + k}{2k} \tag{20}$$

and combining Equations (16) and (20):

$$S = \frac{|V_{F2, rated}| + |V_{F1, rated}|}{2|V_{F1, rated}|} \tag{21}$$

From this expression, we can establish a maximum value of the sag that the proposed TI-IDVR can satisfactorily mitigate:

$$\begin{aligned} sag, max, F1 &= \frac{|V_{F2, rated}| + |V_{F1, rated}|}{2|V_{F1, rated}|}; \quad |V_{F1, rated}| > |V_{F2, rated}| \\ sag, max, F2 &= \frac{|V_{F1, rated}| + |V_{F2, rated}|}{2|V_{F2, rated}|}; \quad |V_{F2, rated}| > |V_{F1, rated}| \end{aligned} \tag{22}$$

where $sag, max, F1$ and $sag, max, F2$ are the maximum sags that can be mitigated at loads 1 and 2, respectively. For example, assuming that $|V_{F1, rated}| = 200$ V and $|V_{F2, rated}| = 150$ V, then $sag, max, F1 = 0.875$; that is, $|V_{F1, sag}| = 25$ V. Considering Equations (4), (10) and (11), we have $|V_{L1, rated}| = |V_{F1, sag}| + |V_{F1, sag}| + |V_{F2, rated}|$; 200 V = 25 V + 25 V + 150 V; this shows that if a sag greater than 87.5% appears, the stability in load voltage is compromised. It should be mentioned that ideal conditions are considered in this analysis; that is, the

voltage losses in the switching elements, the input and output filters of the TI-IDVR, and the injection transformers are not considered.

Now, suppose a voltage swell on feeder 1. Figure 3b shows the relationship of the voltage vectors or voltage phasor in this case. Taking into consideration Figures 2 and 3b, the following equation can be written:

$$\vec{V}_{L1,rated} = \vec{V}_{F1,swell} - \vec{V}_{comp,swell} \quad (23)$$

where $\vec{V}_{L1,rated}$, $\vec{V}_{F1,swell}$ y $\vec{V}_{comp,swell}$ are the voltage vectors for load voltage 1, feeder 1 voltage (with swell), and compensation voltage injected by TI-IDVR, respectively. Following the reasoning used for the voltage sag, we can write the absolute value of the offset voltage $\left| \vec{V}_{comp,swell} \right|$ as follows:

$$\left| \vec{V}_{comp,swell} \right| = aMV_{dc} \quad (24)$$

The value per unit of the voltage swell ($V_{swell,pu}$) based on the nominal value of the load voltage is as follows:

$$V_{swell,pu} = 1 - \left| V_{F1,swell,pu} \right| \quad (25)$$

Now, assuming that the voltages $\vec{V}_{L1,rated}$ and $\vec{V}_{F1,swell}$ are in phase, Equation (23) can be written as follows:

$$\left| V_{L1,rated} \right| = \left| V_{F1,swell} \right| - \left| V_{comp,swell} \right| \quad (26)$$

Considering $\left| V_{L1} \right| = \left| V_{L1,rated} \right|$, Equation (26) can be written as follows:

$$1 = \left| V_{F1,swell,pu} \right| - \left| V_{comp,swell,pu} \right| \quad (27)$$

Combining Equations (24), (25) and (27) we can write:

$$V_{swell,pu} = aMV_{dc,pu} \quad (28)$$

The maximum value of a voltage swell that can be compensated for can be obtained considering $M = 1$. In this way, we can write:

$$V_{swellmax,pu} = aV_{dc,pu} \quad (29)$$

For a DVR under this configuration, the voltage on the virtual dc-link can be estimated by $V_{dc,pu} = \left| V_{F1,pu} \right|$; then, Equation (23) can be written as:

$$V_{swellmax,pu} = a \left| V_{F1,pu} \right| \quad (30)$$

This equation indicates that a DVR in this configuration is capable of compensating for any voltage level that exceeds the rated voltage of the load. For this reason, the proposed TI-IDVR behaves like a conventional DVR in the presence of a voltage swell.

4. CSI Space Vector Pulse Width Modulation

To compensate for the disturbances that occur in the feeders, the CSIs must synthesize the appropriate voltages to be injected into the faulty grid and thus mitigate them. CSIs take voltage from the virtual dc-link and transform it into an appropriate compensation voltage. To do this, the switching elements of the CSIs must turn on and off in a suitable sequence. The space vector pulse width modulation technique is used to obtain the switching on and off sequence of the commutation elements. This technique has been widely adopted to generate the trigger signals of the commutation elements of the inverters

in the DVRs [34–36]. Figure 4 shows the vector representation in the complex space of the active states used by the CSI to form the desired voltage.

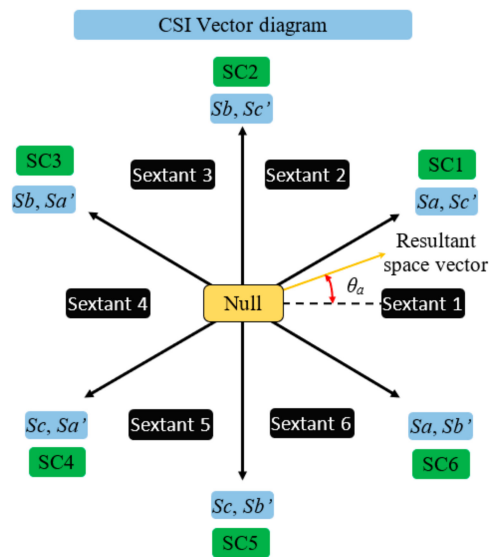


Figure 4. Space vector representation of the active states of the CSI.

Sextant 1 is delimited by the active States of Commutation (SC) SC6 and SC1. These active states correspond to the line voltages v_{ab} and v_{ac} , respectively, and the angle θ_a of the resultant vector in vector space has the range $-\pi/6 \leq \theta_a \leq \pi/6$. In this way, the line voltages are obtained from the voltage in the virtual dc-link by commuting the switches $S_a, S_{b'}$ and $S_a, S_{c'}$ of the inverter. The phase angle orientation of the CSI output voltages is synchronized with the difference between the phase angle of the reference voltages and the phase angle measured on the load. Three-phase output voltages are defined by:

$$\begin{aligned} v_a &= V_{om} \cos \theta_a, \quad v_b = V_{om} \cos \theta_b, \quad v_c = V_{om} \cos \theta_c \\ \theta_a &= \omega t, \quad \theta_b = \theta_a - 2\pi/3, \quad \theta_c = \theta_a + 2\pi/3 \\ v_a + v_b + v_c &= 0 \end{aligned} \tag{31}$$

where V_{om} is the amplitude of the output voltages and θ_a, θ_b and θ_c are the phase angles.

When the load reference voltages and the line voltages are in phase, the duty cycles d_{o1} and d_{o2} for switches $S_{b'}$ and $S_{c'}$ in sextant 1 are determined by:

$$\begin{aligned} -\cos \theta_b / \cos \theta_a - \cos \theta_c / \cos \theta_a &= 1 \\ d_{o1} = -\cos \theta_b / \cos \theta_a, \quad d_{o2} &= -\cos \theta_c / \cos \theta_a \end{aligned} \tag{32}$$

d_{o1} and d_{o2} can be calculated similarly for the other five sextants.

The voltage in the virtual dc-link in sextant 1 is determined by:

$$v_{dlink} = d_{o1}v_{abref} + d_{o2}v_{acref} \tag{33}$$

where v_{abref} and v_{acref} are the reference voltages for the load voltages v_{ab} and v_{ac} , respectively. The voltage in the virtual dc-link in the other five sextants is calculated in a similar way.

5. Carrier Based PWM with Double Reference Algorithm for the TTI-MC

The CB-PWM modulation technique has been widely adopted for the generation of trigger signals in electronic power converters. In [37,38], the CB-PWM technique is used with two references for the purpose of integrating two power generators into the power grid. In this work, we use the MCB-PWM with two modified references to integrate two feeders with their respective loads to a TI-IDVR that can be used in a multi-feeder system or in a CPP.

The MCB-PWM with double reference implemented for TTI-MC modulation employs two sets of reference signals that share a triangular carrier signal. One set of the reference signals corresponds to feeder 1 and the other to feeder 2. The set of reference signals corresponding to feeder1 is placed above the set of signals corresponding to feeder 2. For clarity, we will call phase *a*, phase *b* and phase *c* the three phases of feeder 1; the three phases of feeder 2 will be referred to as phase *r*, phase *y* and phase *w*.

The MCB-PWM process with double references implemented to generate the trigger signals for the switches of a branch of the TTI-MC is shown in Figure 5. The upper (v_{ra}) and lower (v_{rr}) reference signals are compared with the signal triangular carrier (v_{tri}) to obtain the trigger signals of switches S1 and S3. To obtain the trigger signal of switch S2, the logical operator XOR is used between signals S1 and S3. The ratio of the trigger signals can be written functionally as follows:

$$S_1 = \begin{cases} 1, & v_{ra} \geq v_{tri} \\ 0, & v_{ra} < v_{tri} \end{cases} \quad S_3 = \begin{cases} 1, & v_{rr} \leq v_{tri} \\ 0, & v_{rr} > v_{tri} \end{cases} \quad (34)$$

$$S_2 = S_1 \text{ XOR } S_3$$

where v_{ra} and v_{rr} are the upper and lower modulation reference signals that correspond to phase *a* of feeder 1 and phase *r* of feeder 2. v_{tri} is the triangular carrier signal. d_1 and d_3 are the duty cycles for switches S1 and S3. The reference signals are given by:

$$v_{ra} = \frac{m_{i1} \cos(\omega_1 t + \theta_a) + V_{off1}}{v_{dlink}} + V_{offup} \quad (35)$$

$$v_{rr} = \frac{m_{i2} \cos(\omega_2 t + \theta_r) + V_{off2}}{v_{dlink}} + V_{offdown} \quad (36)$$

where m_{i1} and m_{i2} are the modulation indices, ω_1 and ω_2 are the angular frequencies, θ_a and θ_r are the phase angles of the upper and lower input voltages, and V_{off1} and V_{off2} are the compensation variables utilized to improve the modulation indices, which are given by:

$$v_{off1} = -0.5(\max(v_{ra}, v_{rb}, v_{rc}) + \min(v_{ra}, v_{rb}, v_{rc})) \quad (37)$$

$$v_{off2} = -0.5(\max(v_{rr}, v_{ry}, v_{rw}) + \min(v_{rr}, v_{ry}, v_{rw})) \quad (38)$$

where v_{ra} , v_{rb} and v_{rc} are the reference voltages of feeder 1, and v_{rr} , v_{ry} and v_{rw} are the reference voltages of feeder 2. Finally, V_{offup} and $V_{offdown}$ are the offset signals (up and down) that prevent crossing between the reference signal sets. It should be mentioned that the sum of the modulation indices must be less than or equal to 1 for each of the sets of the reference signals if the frequencies of the two feeders are different [37].

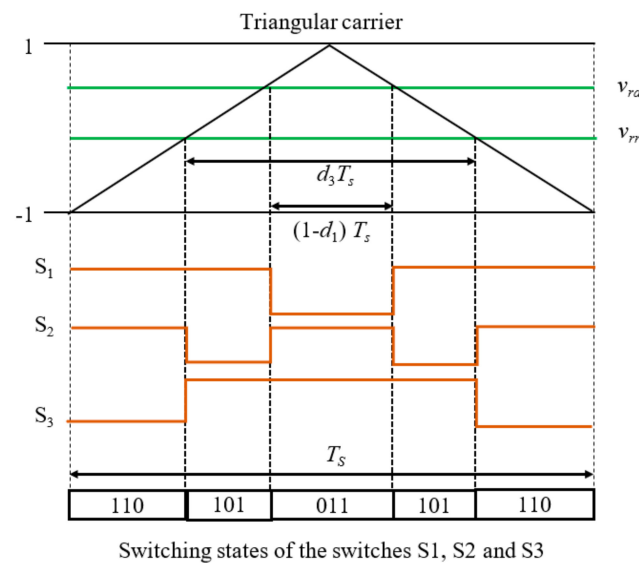


Figure 5. Carrier-based pulse width modulation (MCB-PWM) with double reference scheme for one branch of the TTI-MC. Where, T_s is the period of the triangular carrier signal and d_3 and d_1 are the duty cycles of switches S3 and S1, respectively.

6. TI-IDVR Control Algorithm

The control objectives of this algorithm are the following:

- The TI-IDVR must keep the load voltages stable at their nominal values despite the different types of disturbances (balanced and unbalanced sags and swells, voltage distortion and voltage interruption) that arise in the feeders.
- Have a good targeting of the input currents to the TI-IDVR.
- Hold the voltage waveforms of the feeders and the loads as close as possible to the sinewave.
- Maintain a power factor as close as possible to the unit in the feeders.

The control algorithm presented meets the control objective of producing currents and voltages as close as possible to the sinewave at the input terminals of the TI-IDVR and performs a satisfactory compensation of the load voltages. By implementing this control algorithm, the TI-IDVR compensates for the disturbance present in the load with a good dynamic response. It should be mentioned that the topology of the TTI-MC and its control algorithm implemented in this work allow for a unit power factor at the terminals of the two feeders.

Consider the following scenario for a practical application. Assume a multi-feeder system or a CPP with two feeders where each of the feeders has its own sensitive load. The TI-IDVR is connected to the two feeders so that one of the inputs of the TI-IDVR is connected to feeder 1 and the other is connected to feeder 2. In this way, the TI-IDVR can integrate the power of the two feeders to maintain the voltage of the loads at their nominal value. When there is a voltage sag in feeder 1, it is reflected in the load voltage 1. Then, the TI-IDVR takes power from both feeders to hold load voltage 1 at its nominal value.

On the other hand, if a severe event manifests as a voltage interruption in any of the feeders, then the TI-IDVR behaves as a reconfiguration device and takes power from the healthy feeder to maintain the nominal values of the load voltage for the duration of the event. When there is no short-term disturbance in the feeders, but there is a voltage distortion or imbalance, the TI-IDVR can cope with these events and in this way, and the operating time of the TI-DVR is optimized.

The topology of the TI-IDVR is constituted of a TTI-MC and two CSIs. In this way, the control algorithm can be divided into two parts that are synchronized with each other: (a) the control of the CSIs, and (b) the control of the TTI-MC.

6.1. CSI Control Algorithm

The voltage in the loads can be compensated for efficiently in the reference frame dq even in the presence of voltage disturbances in the feeders. The structure of the control and modulation algorithm implemented to govern the switching on and off of the commutation elements of the CSIs is shown in Figure 6.

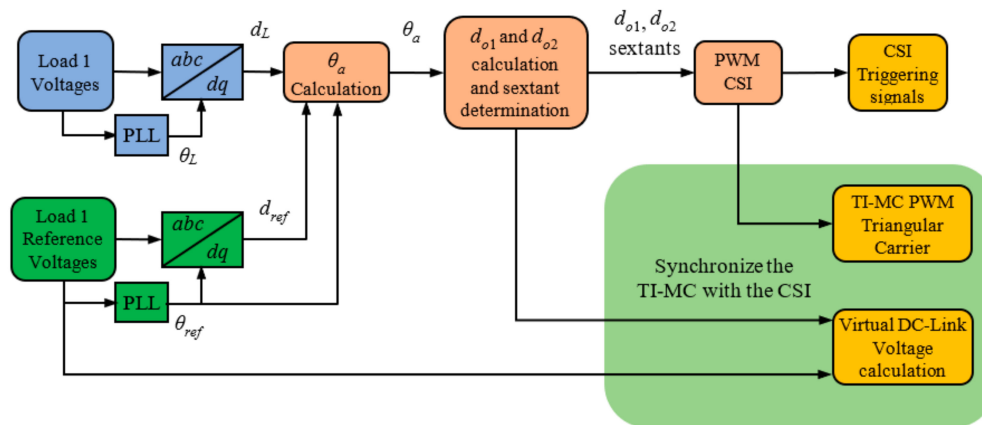


Figure 6. CSI control algorithm.

The control algorithm for CSI 1 and CSI 2 is the same. For this reason, only the control algorithm for CSI 1 is addressed in this description. The inputs to the control algorithm are load voltage 1 and the reference voltage of load 1. The phase angle information (θ_L and θ_{ref}) of both voltages is obtained by means of a Phase-Locked Loop (PLL). The active component of both voltages (d_L and d_{ref}) is obtained by performing the abc - dq transformation using the phase angle information obtained above. The active components (d_L and d_{ref}) of the load and reference voltages are compared to determine if the event is a voltage sag or a voltage swell. With this information, the phase angle of the reference voltage is adjusted to obtain the phase angle θ_a . As shown in Figure 4, the angle θ_a describes the phase orientation of the voltage vectors that are required for disturbance compensation in the complex space. The phase angle θ_a provides the necessary information to determine the corresponding sextant in the complex space and to calculate the switching functions d_{o1} and d_{o2} in each of the sextants using Equation (32). To generate the trigger signals, the switching functions d_{o1} and d_{o2} are compared with a sawtooth signal in the CSI PWM. The sextant defined by angle θ_a determines the switching elements of the CSI that will be turned on and off so that the CSI synthesizes the appropriate line voltages.

To synchronize the TTI-MC with the CSI, the control algorithm performs two functions that are very important for this purpose: a) it generates the triangular carrier signal for the MCB-PWM of the TTI-MC, and b) it calculates the dc-link virtual voltage of the TI-IDVR. The triangular carrier signal is generated in the PWM of the CSI. The voltage value in the virtual dc-link depends directly on the phase voltages of the reference voltage of the load, the sextant determined by the phase angle θ_a , and the switching functions d_{o1} and d_{o2} . The voltage in the virtual dc-link is calculated using Equation (33).

Compared to [12], this paper adds a “selective control” based on “decision rules” that allows for connecting or disconnecting the feeders to the TT-IDVR according to the present disturbance. This allows for different modes of operation of the TTI-IDVR and to connect the feeders to the TTI-IDVR only when necessary. This has the benefit of more efficient use of the power delivered by the feeders to the TI-IDVR, and no power is taken from the feeder without failure when it is not needed. Furthermore, this is a feature that other IDVRs lack [15–22]. The inputs to the decision rules are the active powers of the load voltage (d_L) and the load reference voltage (d_{ref}). The outputs of the decision rules correspond to switches SF1 and SF2 (Figure 2) that connect or disconnect feeders 1 and 2, respectively.

The decision rules for connecting or disconnecting the feeders with respect to the voltages of load 1 are as follows:

For a swell on feeder 1:

IF $d_L > 1.05 * d_{ref}$ THEN SF1 = 1, SF2 = 0; (connects feeder 1 and disconnects feeder 2)

For a sag on feeder 1:

IF $d_L < 0.95 * d_{ref}$ THEN SF1 = 1, SF2 = 1; (connect both feeders)

The decision rules for connecting or disconnecting the feeders with respect to the voltages of load 2 are similar to those shown for load 1.

6.2. TTI-MC Control Algorithm

With this control algorithm, it is guaranteed that the voltage level in the virtual dc-link is adequate so that the CSIs can compensate for the disturbances that appear in the feeders. The TTI-MC integrates the two feeders to the TI-IDVR and acquires power from both grids to supply power to the CSIs through the virtual dc-link. Figure 7 shows the modulation and control scheme of the TTI-MC.

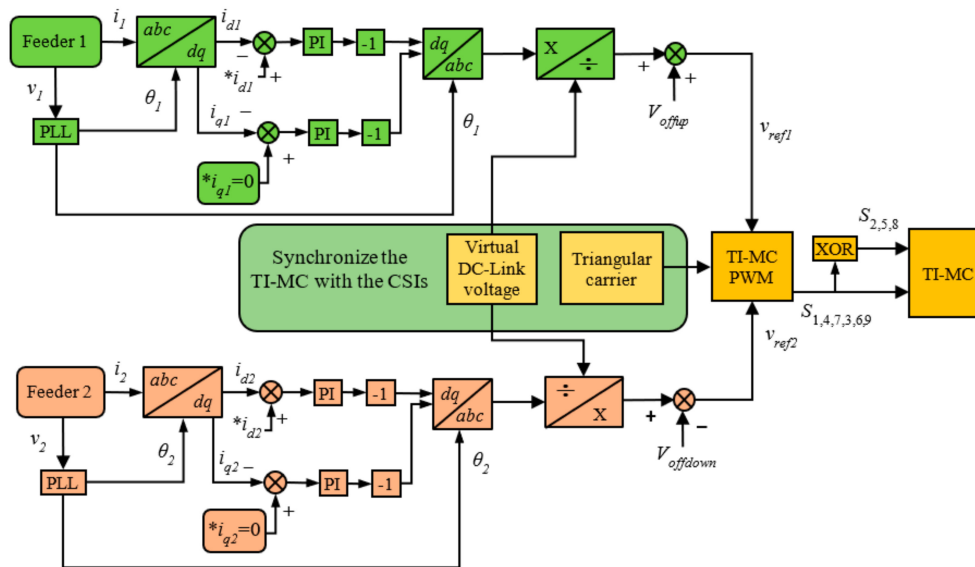


Figure 7. TTI-MC control algorithm and modulation.

To ensure good current targeting and a power factor close to the unit in both feeders, their currents (i_1 and i_2) and voltages (v_1 and v_2) are measured. By focusing attention on feeder 1, its phase angle θ_1 is obtained by means of a PLL. θ_1 is used when performing the abc - dq transformation of the currents measured in feeder 1. By using θ_1 in the transformation, it is guaranteed that the d -axis of the current aligns with the voltage vector of the same feeder. The reference of the reactive current is set to zero; $*i_{q1} = 0$ to have a unit power factor. To control the active and reactive currents of the feeder, Proportional-Integral (PI) controllers are used. Subsequently, the dq - abc transformation synchronized with the angle θ_1 is used to obtain the three-phase set of modulation references for feeder 1. This set of reference signals is divided by the virtual dc-link voltage calculated in the algorithm of CSI control.

To prevent the reference set of feeder 1 from crossing with the reference set of feeder 2, the compensation voltages V_{offup} and $V_{offdown}$ are added. V_{offup} moves the reference set of feeder 1 up and $V_{offdown}$ moves the reference set of feeder 2 down.

The trigger signals of the TTI-MC are generated using the CB-PWM technique with double reference. This technique compares the reference set of feeder 1 (v_{ref1}) and the reference set of feeder 2 (v_{ref2}) with the triangular carrier constructed in the PWM of the

CSI. By comparing the reference set of feeder 1 (v_{ref1}) with the triangular carrier signal, the on and off times of the switches S1, S4 and S7 are obtained and the on and off times for switches S3, S6 and S9 are obtained by comparing the triangular carrier signal with the reference set of feeder 2 (v_{ref2}). To obtain the trigger signals of switches S2, S5 and S8, the logical operator XOR is used as follows: $S2 = (S1) \text{ XOR } (S3)$.

With this control algorithm, the proposed TI-IDVR has good multi-functional performance and is able to compensate for deep and long-term sags, swells, interruptions, voltage imbalances and harmonic distortion. In addition, this algorithm has additional advantages such as:

- The energy storage capacity to compensate for deep and long-term sags is not a limitation because the power is taken from the two feeders by means of the TTI-MC.
- There are no energy storage devices in the virtual dc-link. Therefore, it is not necessary to measure the voltage on the dc-link for control purposes.
- With this control scheme, the TTI-MC behaves like two Voltage Source Converters (VSCs) and integrates two feeders to the TI-IDVR using only a unified control algorithm. Under a conventional scheme, two VSCs and a controller are needed for each of them.
- The control algorithm for the TI-IDVR used in this work is more compact compared to the control algorithms used in conventional AC-DC-AC two-stage converters with energy storage elements used in IDVRs.

7. Simulation Results and Discussion

In this section, the behavior of the proposed TI-IDVR and its control algorithm is verified through simulations. The complete system was implemented on MATLAB R2015b (64 bits)/Simulink Version 8.6 platform, and the SimPowerSystems library was used. Figure 8 shows the real model implemented in Simulink corresponding to the proposed TI-IDVR of Figure 2. It should be noted that ideal switching elements were used for simulation purposes. This is because the objective of this work is to verify the effectiveness of the proposed TI-IDVR and its modulation scheme. For an experimental implementation, more elements should be considered, especially protection and galvanic isolation at the TTI-MC inputs. Snubber circuits were used to protect the switching elements of the TTI-MC and the CSIs against overvoltages. The resistance and capacitor values for the TTI-MC switching elements were $R = 33 \Omega$ and $C = 333 \mu\text{F}$, and the values for the CSIs were $R = 33 \Omega$ and $C = 10 \mu\text{F}$. In the injection transformers, the ideal Matlab/Simulink transformers with a 1:1 ratio were used. The model for generating the reference voltages of the feeders is shown in Figure 9, and the Simulink model of the control algorithm of the CSIs is shown in Figure 10.

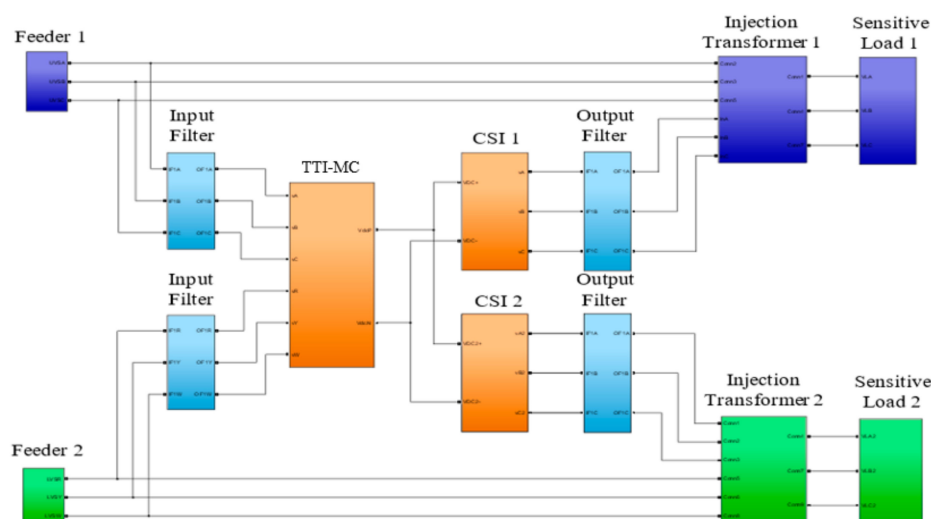


Figure 8. Implemented model in Simulink of the proposed TI-IDVR.

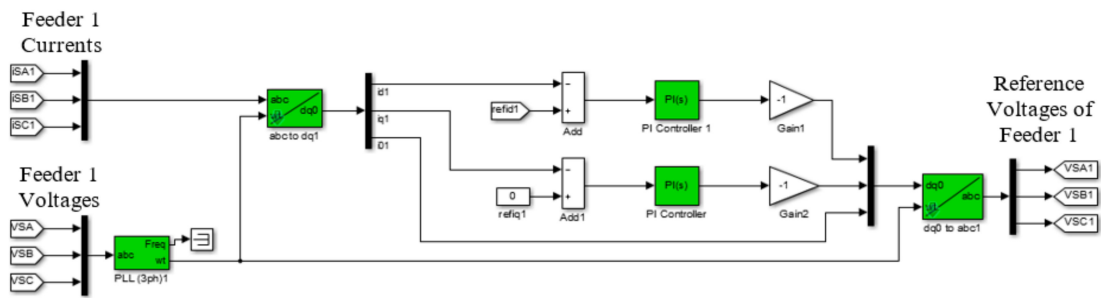


Figure 9. Models for the generation of the reference voltages of feeder 1.

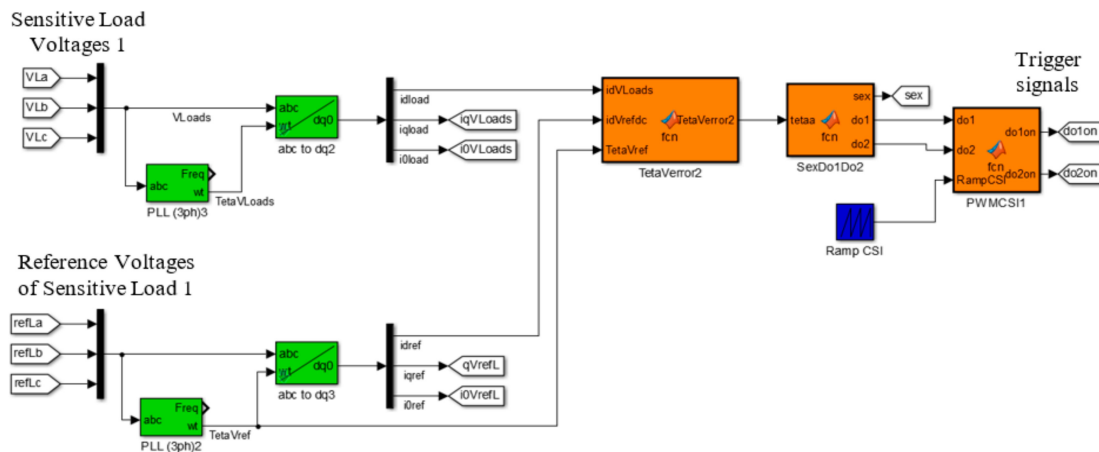


Figure 10. Model of the CSI 1 control algorithm.

The system parameters used in the simulations are shown in Table 1.

Table 1. TI-IDVR simulation parameters.

Quantity/Parameter	Values and Units
Capacitors of the input filters	10 μ F
Resistance of the input filters	50 Ω
Inductors of the input filters	2.2 mH
Output filter capacitor	4.7 μ F
Output filter resistance	100 Ω
Output filter inductor	25 mH
Load resistance	120 Ω
Load inductor	8 mH
Feeder 1 and 2	100 Vp, 60 Hz
Load reference voltages 1 and 2	100 Vp, 60 Hz
CSI switching frequency	3.6 KHz
TTI-MC switching frequency	7.2 KHz
Gains of the PI controllers	$K_p = 30, K_i = 0.001$

K_p and K_i correspond to the proportional and integral gains of the PI controller.

The behavior of the proposed DVR was analyzed for the following study cases:

- Case 1: Voltage sag with harmonic distortion.
- Case 2: Unbalanced voltage swell.
- Case 3: Voltage interruption.

7.1. Case 1: Voltage Sag with Harmonic Distortion

A sag is defined as the decrease in the rms (Root Mean Square) value of the supply voltage, between 0.1 and 0.9 pu, at the feeding frequency and with a duration from 0.5

cycle to 1 min. Voltage distortion in power supplies is one of the most common problems of PQ and has a negative impact on electrical networks and on loads sensitive to voltage variations.

In this section, the performance of the proposed TI-IDVR in the compensation of voltage sags with harmonic distortion in the feeders is verified. To simulate this event, the peak voltage of the feeders is reduced from 100 Vp to 65 Vp and the fifth harmonic with an amplitude of 20% with respect to the fundamental is added.

When the disturbance occurs, the TI-IDVR behaves like an IDVR and draws power from the two feeders to compensate for the disturbance, as well as keeping the voltage on the sensitive load stable. The event occurs on feeder 1 in the 50 ms to 100 ms time interval, and on feeder 2 from 150 ms to 200 ms. The waveforms of the voltages and currents obtained in the simulation are shown in Figures 11 and 12.

Feeder 1 voltages, compensation 1 voltages, load 1 voltages, and the voltage on the virtual dc-link are shown in Figure 11. The figure shows how the voltages of load 1 remain practically at their nominal values despite the disturbance in feeder 1. It can also be seen how effectively the TTI-MC integrates the power from the two feeders to construct the virtual dc-link voltage and thus provides the necessary power to CSI 1 so that it can synthesize the appropriate compensation voltages. In Figure 11, the voltages in feeder 2 and sensitive load 2 remain unchanged in the presence of the disturbance in feeder 1. In the same way, when the voltage sag occurs in feeder 2, the TTI-MC integrates the power of the two feeders, CSI 2 generates the desired injection voltage, and the voltage in load 2 remains unchanged despite the disturbance in feeder 2 as shown in Figure 11.

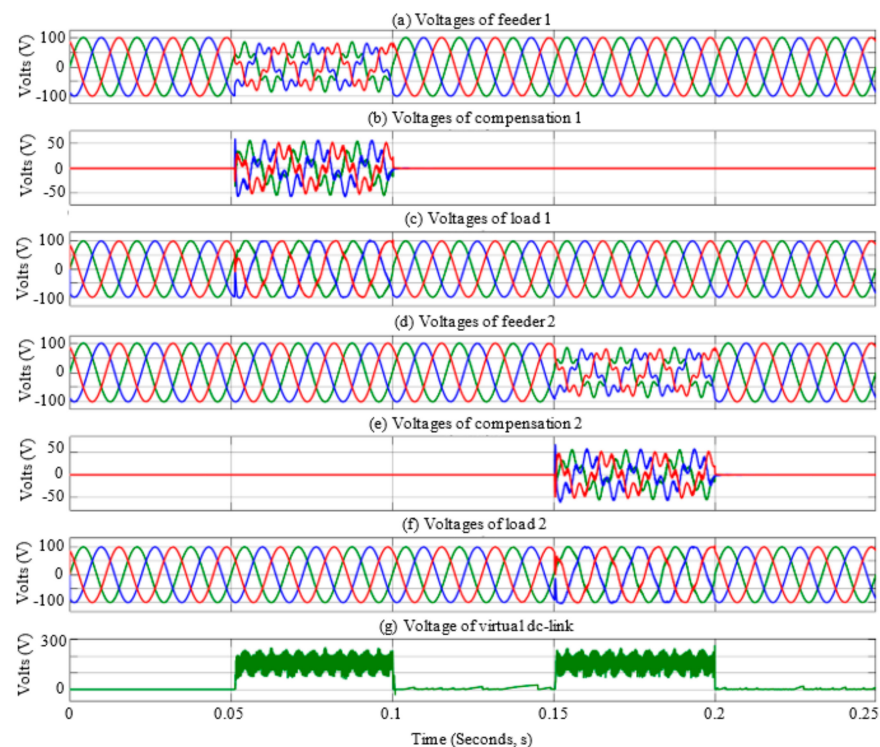


Figure 11. System waveforms in the compensation of voltage sags and harmonic distortion. (a–c) feeder 1 waveforms; (d–f) feeder 2 waveforms; (g) virtual dc-link voltage waveform.

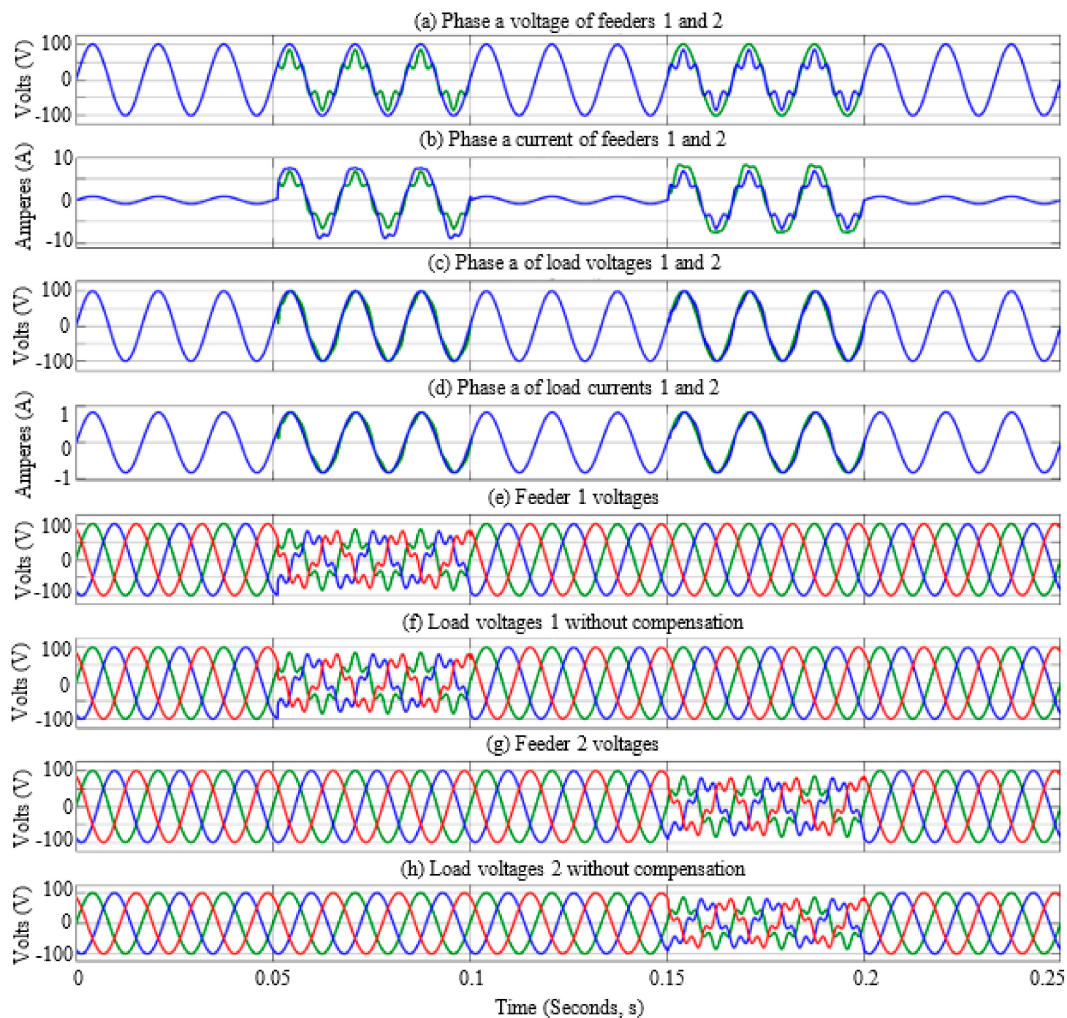


Figure 12. System waveforms in the compensation of voltage sags and harmonic distortion. (a–d) System waveforms (phase *a*); (e–h) system waveforms without TI-IDVR.

Figure 12 shows the phase *a* waveforms of the system. The figure shows that when the disturbance occurs, the voltages and currents in the loads remain practically unchanged despite the disturbance in the feeder. In addition, the voltages and currents of both feeders are in phase. However, in the presence of the disturbance, the TI-IDVR demands a higher current from the feeders; this does not represent a disadvantage since the higher current consumption is an inherent characteristic of the configuration of DVRs without energy storage systems when connected on the source side.

Finally, the behavior of the system without the TI-IDVR is shown in Figure 12. Comparing Figures 11 and 12, the effectiveness of the proposed TI-IDVR in compensating for voltage sags and harmonic distortion that occur in the feeders can be seen.

7.2. Case 2: Unbalanced Voltage Swell

A swell is defined as an increase in the rms value of voltage or current of around 1.1 to 1.8 pu, with a duration from 0.5 cycles to 1 min. It is said that a three-phase voltage system is unbalanced if the magnitudes of the phase or line voltages are different from each other.

In this section, the performance of the proposed TI-IDVR in the compensation of unbalanced voltage swell in the feeders is verified. To simulate these disturbances, the peak voltage of the feeders is increased from 100 V_p to 115 V_p in phase *a*, to 130 V_p in phase *b*, and to 145 V_p in phase *c*.

When this disturbance arises, the TI-IDVR behaves like a conventional DVR. That is, the TTI-MC only takes power from the feeder that presents the unbalanced swell voltage for the TI-IDVR to perform the proper compensation. It is worth mentioning that this mode of operation is an important feature of the proposed TI-IDVR, unlike other IDVRs that draw power from the feeder without failure to compensate for the disturbance.

The voltage and current waveforms of the entire system are shown in Figures 13 and 14. Figure 14 shows the waveforms of the system without TI-IDVR. The disturbance occurs at feeder 1 in the 50 ms to 100 ms time interval as shown in Figure 13. In this time interval, the TTI-MC only takes power from feeder 1 and transfers it to the virtual dc-link. The CSI 1 takes this power and builds the compensation voltage as shown in Figure 13. In this way, the unbalanced voltage swell is successfully compensated and the voltage at sensitive load 1 remains stable. The behavior of the TI-IDVR in compensating for this disturbance in feeder 2 is shown in Figure 13. The difference is that the TTI-MC draws power from feeder 2, and CSI 2 synthesizes the proper injection voltage to adequately compensate for the unbalanced voltage swell in feeder 2 and keeps the voltage at sensitive load 2 stable.

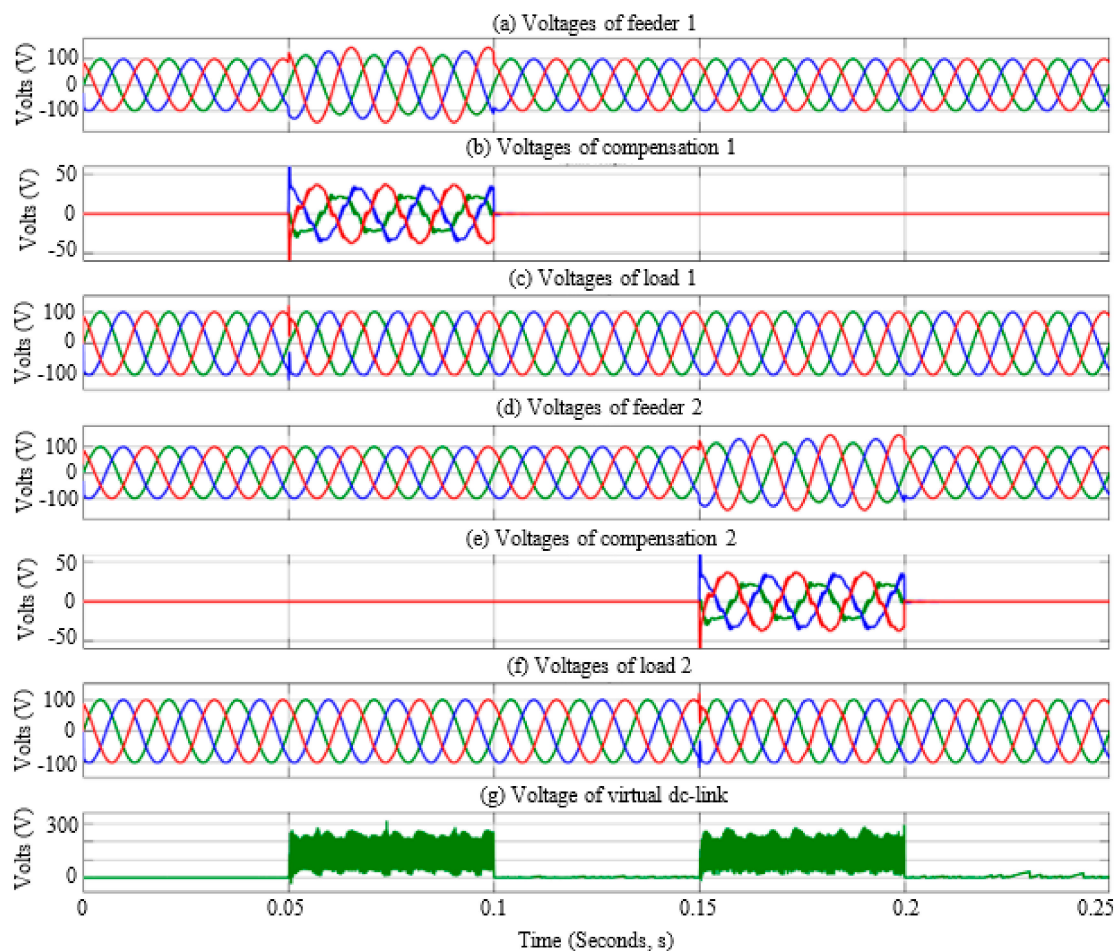


Figure 13. System waveforms in the unbalanced voltage swell compensation. (a–c) Waveforms of feeder 1; (d–f) feeder 2 waveforms; (g) virtual dc-link voltage waveform.

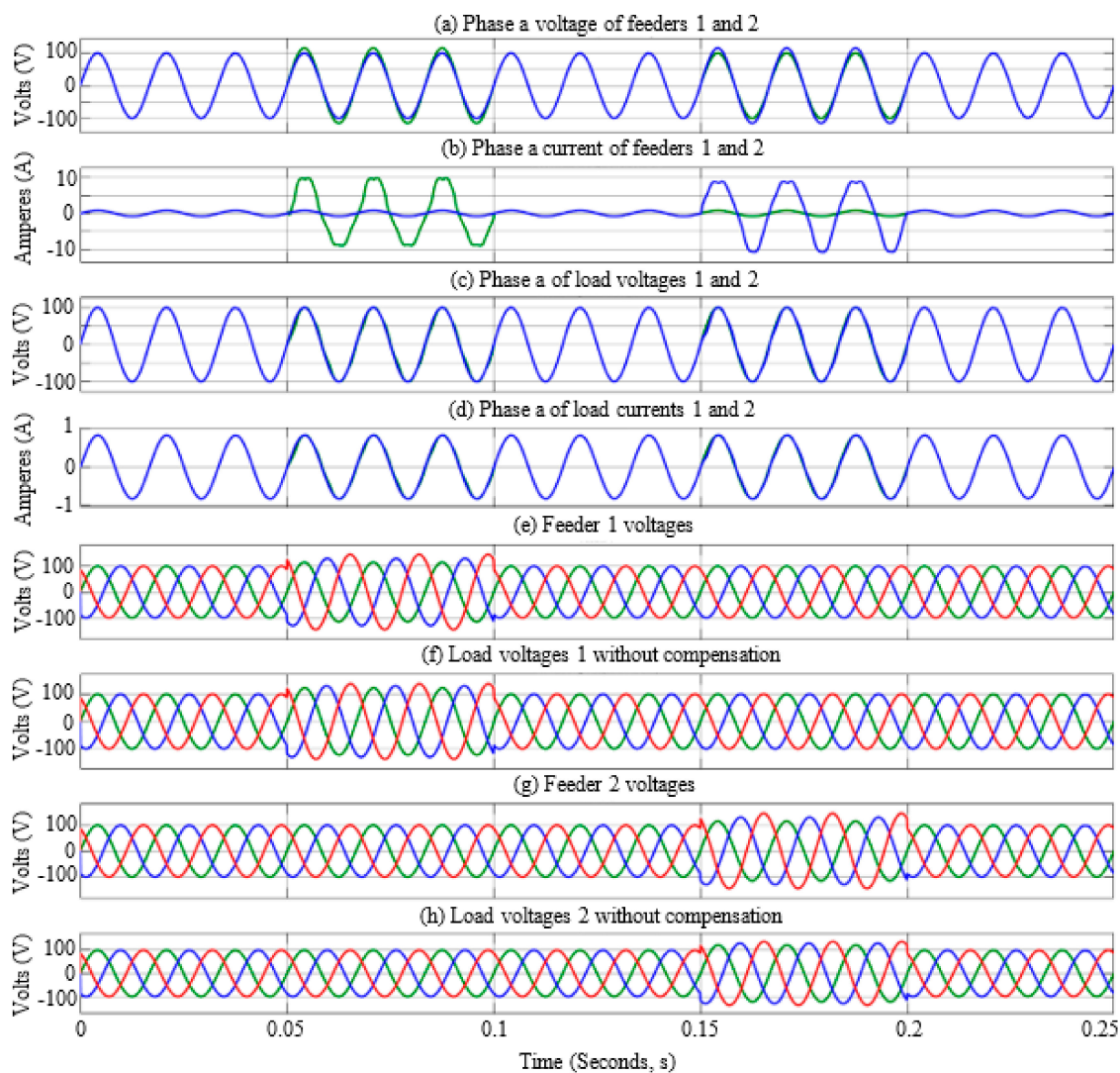


Figure 14. System waveforms in the unbalanced voltage swell compensation. (a–d) System phase *a* waveforms; (e–h) system waveforms without a TI-IDVR.

The phase *a* voltage and current waveforms of the system are shown in Figure 14. When the event occurs in feeder 1, the voltages and currents of feeder 2 and sensitive load 2 remain unchanged. Furthermore, it can be clearly seen in the figure that the voltage and current in sensitive load 1 remain stable despite the disturbance. The figure also shows that the voltages and currents in the feeders and the sensitive loads are in phase. Therefore, it can be concluded that the proposed TI-IDVR is capable of maintaining a unit power factor in feeders and sensitive loads despite this type of feeder disturbance.

System behavior without a TI-IDVR is shown in Figure 14. Comparing Figures 13 and 14, the effectiveness of the proposed TI-IDVR in the compensation of unbalanced voltage swells can be appreciated.

7.3. Case 3: Voltage Interruption

An interruption occurs when the supply voltage or load current decreases to less than 0.1 pu for a period of time of less than 1 min.

In this operation mode, the TI-IDVR has the functionalities of a compensation device and also of a network reconfiguration device. When the interruption appears in any of the feeders, the TI-IDVR draws the necessary power from the feeder without failure to keep the voltages and currents of the sensitive load corresponding to the failed feeder stable. In this way, the proposed TI-IDVR behaves like a reconfiguration device that transfers power

from a faultless grid to a faulty grid. Needless to say, this is a feature that conventional IDVRs lack.

To simulate a voltage interruption in the feeders, the peak voltage of all phases is reduced from 100 to 5 Vp for 50 ms. The waveforms of system voltages and currents are shown in Figures 15 and 16. In the 50 to 100 ms time interval, the voltage interruption in feeder 1 is simulated. The voltage interruption of feeder 2 is simulated in the time range of 150 to 200 ms.

In this case, in order to hold the voltage stable in sensitive load 1, the TI-IDVR transfers the necessary power from feeder 2 to feeder 1. The voltage interruption in feeder 1, the virtual dc-link voltage and the injected voltage are shown in Figure 15. The figure shows that the TTI-MC transfers the power from the feeder without fail to the virtual dc-link. The CSI 1 takes this power and synthesizes the compensation voltage. The peak value of the injected voltage is 95 Vp. The figure shows that the voltages of load 1 remain stable at their nominal values despite the voltage interruption. Figure 15 shows a similar behavior of the TI-IDVR when the disturbance occurs in feeder 2.

Figure 16 shows the current and voltage waveforms of phase *a* of the feeders and loads. When the interruption occurs in feeder 1, the voltage in feeder 2 remains stable. However, the TI-IDVR demands more current from the feeder without failure. The figure also shows that the voltages and currents in the feeders and the sensitive loads are in phase. Therefore, it can be concluded that the proposed TI-IDVR is capable of satisfactorily compensating for voltage interruptions, and can also maintain a unit power factor in the feeders and loads despite the interruption in the feeders.

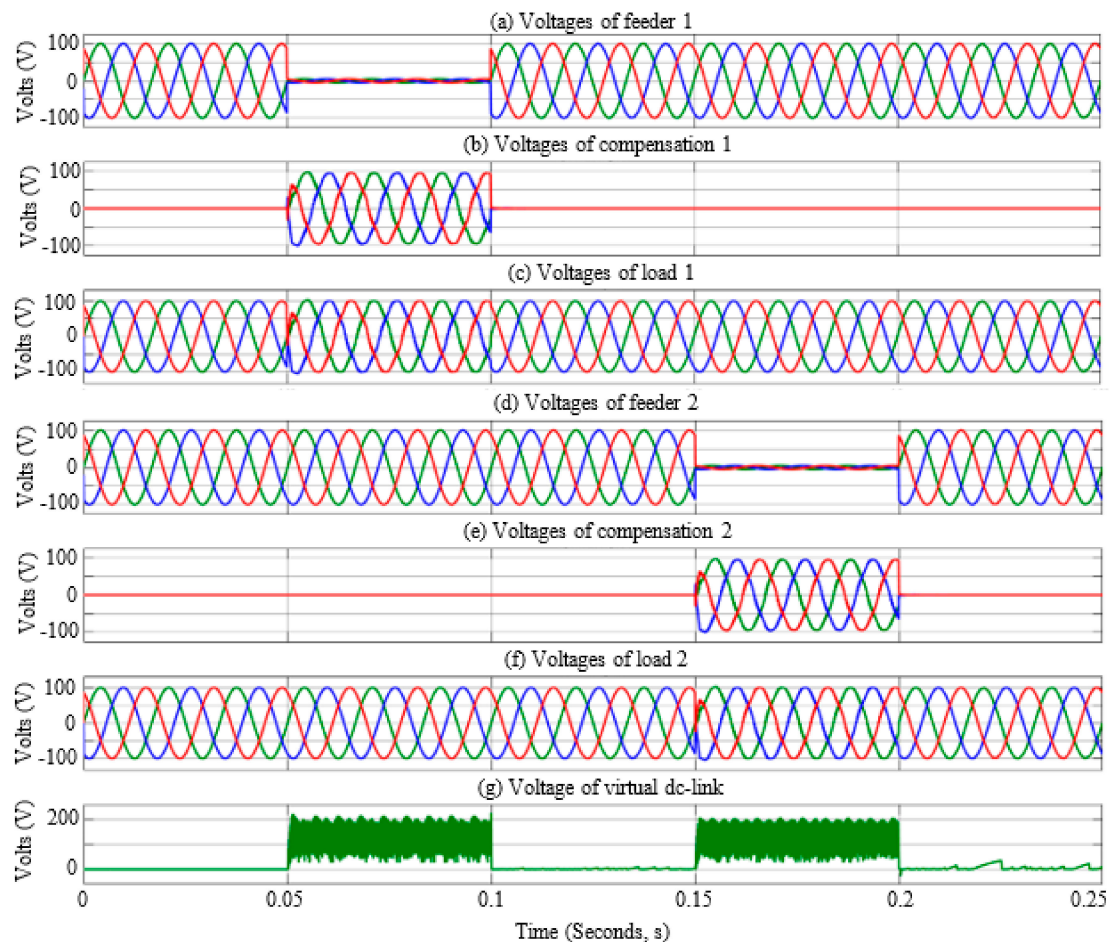


Figure 15. System waveforms in the voltage interruption compensation. (a–c) Waveforms of feeder 1; (d–f) waveforms of feeder 2; (g) virtual dc-link voltage waveform.

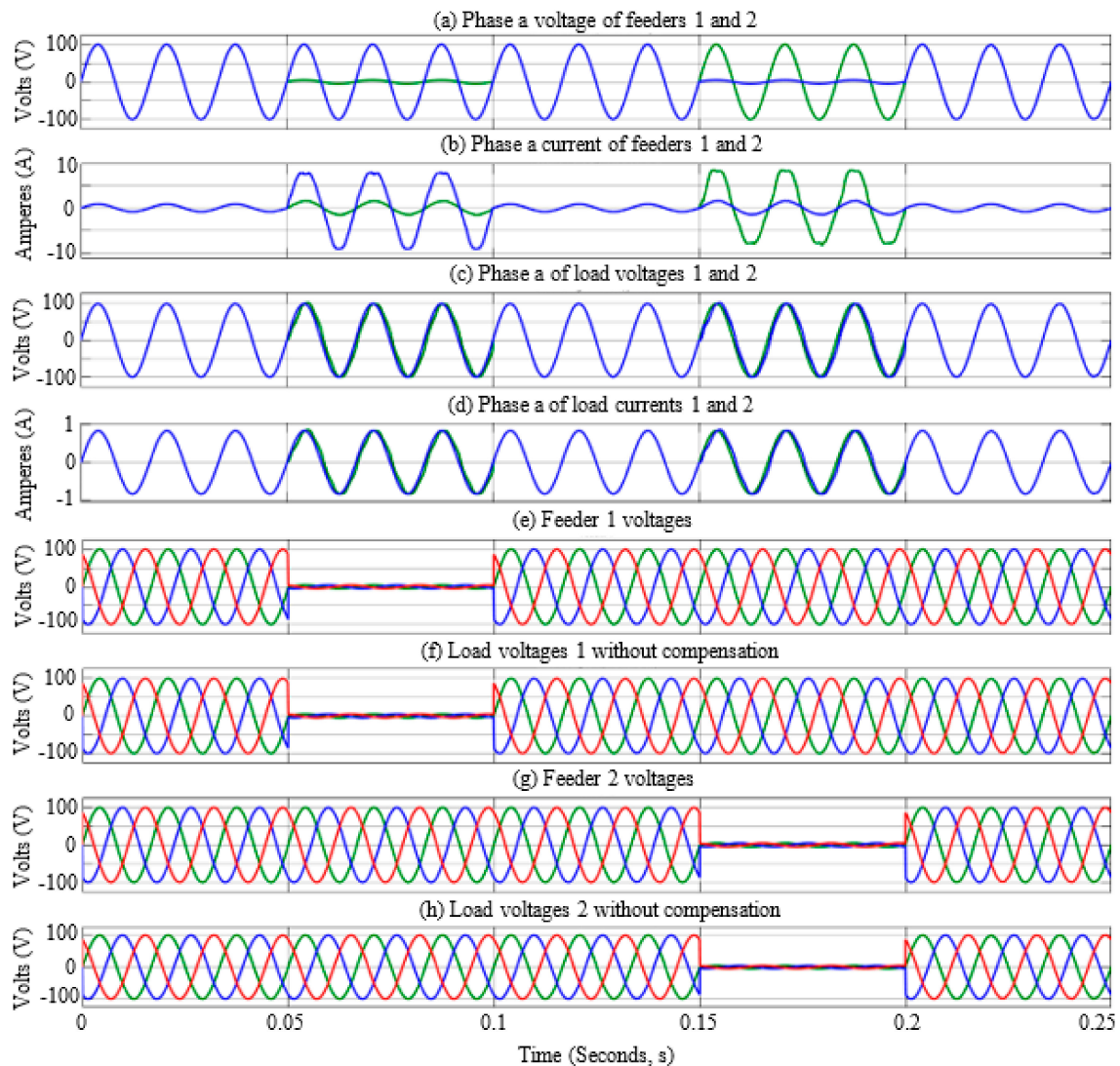


Figure 16. System waveforms in the voltage interruption compensation. (a–d) System phase *a* waveforms; (e–h) system waveforms without TI-IDVR.

System waveforms without TI-IDVR are shown in Figure 16. Comparing the waveforms of voltages and currents of the system shown in Figures 15 and 16, the good performance of the proposed TI-IDVR is evident even in the compensation of severe disturbances, such as voltage interruption, in the feeders.

7.4. Summary of the Results

The simulations shown in the previous sections and their respective discussion demonstrate that the proposed TI-IDVR has the ability to mitigate the disturbances that appear in the two feeders of the system and maintain the voltages and currents of the sensitive loads at their nominal values.

An important feature of the TI-IDVR is the fact that it can work in different modes of operation to perform disturbance compensation as mentioned below.

7.4.1. The TI-IDVR as an IDVR

The TTI-MC draws power from the two feeders to compensate for the disturbance. In this way, the TI-IDVR greatly extends its compensation range and can cope with deep and long-term voltage sags without the need for additional energy storage devices that would increase its cost and risk of failure. In addition, the TI-IDVR behaves like a compensation

device and it also has the performance of a reconfiguration device. When there is a voltage interruption in one of the feeders, the TI-IDVR takes the necessary power from the feeder without failure to compensate for the disturbance and keeps the voltages and currents of the load in the faulty grid stable at their nominal values.

7.4.2. TI-IDVR as a conventional DVR

When a voltage swell occurs, the TI-IDVR constructs the compensation voltage with the excess power in the faulty feeder. That is, the TTI-MC does not draw power from the feeder without failure to perform the disturbance compensation.

The advantages and characteristics of the proposed topology, its control algorithm and its modulation scheme are summarized below:

- The implemented control algorithm allows the TI-IDVR to have a multi-functional capacity to synthesize the appropriate voltages for the compensation of different types of disturbances in the feeders.
- The control algorithm of the TI-IDVR is more compact compared to the control algorithms used in conventional IDVRs where the voltage level in the dc-link has to be controlled.
- The calculated voltage of the dc-link is obtained according to the reference voltages of the loads and the switching functions of the PWM CSIs. This allows for a natural and optimal synchronization and power transfer between the TTI-MC and the CSIs.
- The synchronization between the TTI-MC and the CSIs contributes to the sinusoidal waveforms of the currents in the feeders.
- Unlike other works, the proposed topology and its control algorithm allow for a unit power factor in the feeders and the loads even in the presence of deep and long-term voltage sags, as well as in voltage interruptions.

The incorporation of the TTI-MC into the topology of the IDVR results in the multi-functional behavior of the TI-IDVR. The simulation results show the efficiency and validity of the proposed topology.

8. Conclusions

In this paper, the performance of the TI-IDVR based on a TTI-MC was analyzed. The proposed topology has been evaluated in the compensation of different types of PQ problems. The control algorithm of the TI-IDVR has the advantage of being more compact compared to the control schemes of conventional IDVRs based on AC-DC-AC converters. An important feature of the proposed TI-IDVR is the ability to transfer power between two feeders in a similar way to a reconfiguration device in a multi-feeder system or in a CPP. In addition, it extends the compensation range of the TI-IDVR compared to conventional IDVRs and improves its overall behavior. This makes it an attractive solution to deal with different types of PQ problems, including severe events such as deep and long-term voltage sags and voltage interruptions.

On the other hand, the proposed TI-IDVR topology presents many development opportunities for future research, including:

- The implementation of a prototype for experimental tests.
- Use as an integration device of distributed energy resources in a microgrid.
- Use as a compensation and reconfiguration device in microgrids and smart grids.
- Use as an interface and compensation device between AC and DC buses in hybrid microgrids.
- Use as an interface between the main network and a microgrid in order to improve their reliability.

Author Contributions: Conceptualization, S.C.Y.-C.; formal analysis, S.C.Y.-C.; investigation, S.C.Y.-C.; methodology, S.C.Y.-C., G.C.-V. and J.M.L.-G.; supervision, G.C.-V. and J.M.L.-G.; validation, G.C.-V. and J.M.L.-G.; writing—original draft, S.C.Y.-C.; Writing—review and editing, S.C.Y.-C., G.C.-V. and J.M.L.-G. All authors have read and agreed to the published version of the manuscript.

Funding: This research was funded by the Program for Teacher Professional Development (PRODEP) grant number ITESI-008.

Conflicts of Interest: The authors declare no conflict of interest.

References

- Electric Power Research Institute (EPRI). *Power Quality in Commercial Buildings*; BR-105018; EPRI: Palo Alto, CA, USA, 1995.
- Koval, D.O.; Hughes, M.B. Canadian national power quality survey: Frequency of industrial and commercial voltage sags. *IEEE Trans. Ind. Appl.* **1997**, *33*, 622–627. [[CrossRef](#)]
- Sabin, D.D.; Electric Power Research Institute (EPRI). *An Assessment of Distribution System Power Quality*; EPRI-TR-106294-V2; EPRI: Palo Alto, CA, USA, 1996.
- Hingorani, N. Introducing custom power. *IEEE Spectr.* **1995**, *32*, 41–48. [[CrossRef](#)]
- Pal, Y.; Swarup, A.; Singh, B.A. Review of compensating type custom power devices for power quality improvement. In Proceedings of the 2008 Joint International Conference on Power System Technology and IEEE Power India Conference, New Delhi, India, 12–15 October 2008; pp. 1–8.
- Praveena, S.; Kumar, B.S. Performance of custom power devices for power quality improvement. In Proceedings of the 2017 IEEE International Conference on Power, Control, Signals and Instrumentation Engineering (ICPCSI), Chennai, India, 21–22 September 2017; pp. 912–917.
- Nielsen, J.G.; Blaabjerg, F. A detailed comparison of system topologies for dynamic voltage restorers. *IEEE Trans. Ind. Appl.* **2005**, *41*, 1272–1280. [[CrossRef](#)]
- İnci, M.; Büyük, M.; Tan, A.; Bayındır, K.C.; Tümay, M. Survey of inverter topologies implemented in dynamic voltage restorers. In Proceedings of the 4th International Conference on Control, Decision and Information Technologies (CoDIT), Barcelona, Spain, 5–7 April 2017; pp. 1141–1146.
- Sadigh, A.K.; Smedley, K.M. Review of voltage compensation methods in dynamic voltage restorer (DVR). In Proceedings of the 2012 IEEE Power and Energy Society General Meeting, San Diego, CA, USA, 22–26 July 2012; pp. 1–8.
- Nielsen, J.G.; Blaabjerg, F.; Mohan, N. Control strategies for dynamic voltage restorer compensating voltage sags with phase jump. In APEC 2001. In Proceedings of the Sixteenth Annual IEEE Applied Power Electronics Conference and Exposition, Anaheim, CA, USA, 4–8 March 2001; pp. 1267–1273.
- Tien, D.V.; Gono, R.; Leonowicz, Z. A Multifunctional Dynamic Voltage Restorer for Power Quality Improvement. *Energies* **2018**, *11*, 1351. [[CrossRef](#)]
- Yáñez-Campos, S.C.; Cerda-Villafaña, G.; Lozano-Garcia, J.M. Two-Feeder Dynamic Voltage Restorer for Application in Custom Power Parks. *Energies* **2019**, *12*, 3248. [[CrossRef](#)]
- Babaei, E.; Kangarlu, M.F. A new topology for dynamic voltage restorers without dc link. In Proceedings of the 2009 IEEE Symposium on Industrial Electronics & Applications (ISIEA 2009), Xian, China, 25–27 May 2009; pp. 1016–1021.
- Zargar, A.; Barakati, S.M. A new dynamic voltage restorer structure based on three-phase to single-phase AC/AC matrix converter. In Proceedings of the 2015 20th Conference on Electrical Power Distribution Networks Conference (EPDC), Zahedan, Iran, 28–29 April 2015; pp. 234–238.
- Farhadi-Kangarlu, M. An interline dynamic voltage restorer using neutral-point-clamped (npc) multilevel converter. *Power Eng. Electr. Eng.* **2018**, *16*, 46–56. [[CrossRef](#)]
- Ratna Kumari, C.; Kishore Kumar, T. Improving the compensation capacity of interline dynamic voltage restorer. *Int. J. Inf. Theory (IJIT)* **2017**, *6*, 1–12.
- Vilathgamuwa, D.M.; Wijekoon, H.M.; Choi, S.S. A Novel Technique to Compensate Voltage Sags in Multiline Distribution System—The Interline Dynamic Voltage Restorer. *IEEE Trans. Ind. Appl.* **2006**, *53*, 1603–1611. [[CrossRef](#)]
- Ngai-Man Ho, C.; Shu-Hung, H. Implementation and Performance Evaluation of a Fast Dynamic Control Scheme for Capacitor-Supported Interline DVR. *IEEE Trans. Power Electron.* **2010**, *25*, 1975–1988.
- Shahabadini, M.; Iman-Eini, H. Improving the Performance of a Cascaded H-Bridge-Based Interline Dynamic Voltage Restorer. *IEEE Trans. Power Deliv.* **2016**, *31*, 1160–1167. [[CrossRef](#)]
- Moradlou, M.; Karshenas, H.R. Design Strategy for Optimum Rating Selection of Interline DVR. *IEEE Trans. Power Deliv.* **2011**, *26*, 242–249. [[CrossRef](#)]
- Vilathgamuwa, D.M.; Wijekoon, H.M.; Choi, S.S. Interline Dynamic Voltage Restorer: A Novel and Economical Approach for Multiline Power Quality Compensation. *IEEE Trans. Ind. Appl.* **2004**, *6*, 1678–1685. [[CrossRef](#)]
- SivaRanjani, S.; Suresh, K. Hybrid interline dynamic voltage restoring and displacement factor controlling device for improving power quality of the distribution. In Proceedings of the 2016 International Conference on Electrical, Electronics, and Optimization Techniques (ICEEOT), Chennai, India, 3–5 March 2016; pp. 4581–4585.
- Padmarasan, M.; Babu, R.S. Analysis of Interline Dynamic Voltage Restoration in Transmission Line. In *Intelligent Computing in Engineering*. In *Advances in Intelligent Systems and Computing*; Springer: Singapore, 2020; pp. 587–595.
- Jabbari, M.; Moradlou, M.; Bigdeli, M. A TLBO Algorithm for Design Optimization of DVRs in an Interline DVR (IDVR). In Proceedings of the 2019 International Aegean Conference on Electrical Machines and Power Electronics (ACEMP) & 2019 International Conference on Optimization of Electrical and Electronic Equipment (OPTIM), Istanbul, Turkey, 2–4 September 2019; pp. 341–346.

25. Moradlou, M.; Bigdeli, M. DVRs Rating Optimization in an Interline DVR (IDVR) Considering Dominant Interval Concept. In Proceedings of the Electrical Engineering (ICEE), Seoul, South Korea, 24–28 June 2018; pp. 1077–1082.
26. Mohammed, B.S.; Rama Rao, K.S.; Ibrahim, R.; Perumal, N. Application of custom power park to improve power quality of sensitive loads. In Proceedings of the IEEE 5th India International Conference on Power Electronics (IICPE), Delhi, India, 6–8 December 2012; pp. 1–6.
27. Ghosh, A.; Joshi, A. The concept and operating principles of a mini custom power park. *IEEE Trans. Power Deliv.* **2004**, *19*, 1766–1774. [[CrossRef](#)]
28. Seung-Min, S.; Jin-Young, K.; In-Dong, K. New three-phase static transfer switch using AC SSCB. In Proceedings of the 2018 International Power Electronics Conference, Niigata, Japan, 20–24 May 2018; pp. 3229–3236.
29. Aghazadeh, A.; Noroozian, R.; Jalilvand, A.; Haeri, H. Combined operation of dynamic voltage restorer with distributed generation in custom power park. In Proceedings of the 10th International Conference on Environment and Electrical Engineering, Rome, Italy, 1–7 May 2011; pp. 1–4.
30. Mahmood, T.; Choudhry, M.A. Application of static transfer switch for feeder reconfiguration to improve voltage at critical locations. In Proceedings of the 2006 IEEE/PES Transmission & Distribution Conference and Exposition: Latin America, Caracas, Venezuela, 15–18 August 2006; pp. 1–6.
31. Szcześniak, P.; Kaniewski, J.; Jarnut, M. AC–AC power electronic converters without DC energy storage: A review. *Energy Convers. Manag.* **2015**, *92*, 483–497. [[CrossRef](#)]
32. Soliman, H.; Wang, H.; Blaabjerg, F. A Review of the Condition Monitoring of Capacitors in Power Electronic Converters. *IEEE Trans. Ind. Appl.* **2016**, *6*, 4976–4989. [[CrossRef](#)]
33. Rohouma, W.; Balog, R.; Peerzada, A.; Begovic, M. Reactive Power Compensation of Time-Varying Load Using Capacitor-less D-STATCOM. In Proceedings of the 2019 10th International Conference on Power Electronics and ECCE Asia, Busan, Korea, 27–31 May 2019; pp. 2296–2301.
34. Zhan, C.; Ramachandaramurthy, V.K.; Arulampalam, A.; Fitzer, C.; Kromlidis, S.; Bames, M.; Jenkins, N. Dynamic voltage restorer based on voltage-space-vector PWM control. *IEEE Trans. Ind. Appl.* **2001**, *37*, 1855–1863. [[CrossRef](#)]
35. Rosli, O.; Rahim, N.A. Implementation and control of a dynamic voltage restorer using Space Vector Pulse Width Modulation (SVPWM) for voltage sag mitigation. In Proceedings of the 2009 International Conference for Technical Postgraduates (TECHPOS), Kuala Lumpur, Malaysia, 14–15 December 2009; pp. 1–6.
36. Prakash, N.; Jacob, J.; Reshmi, V. Comparison of DVR performance with Sinusoidal and Space Vector PWM techniques. In Proceedings of the 2014 Annual International Conference on Emerging Research Areas: Magnetics, Machines and Drives (AICERA/iCMMD), Kottayam, India, 24–26 July 2014; pp. 1–6.
37. Liu, X.; Wang, P.; Loh, P.C.; Blaabjerg, F. A three-phase dual-input matrix converter for grid integration of two ac type energy resources. *IEEE Trans. Ind. Electron.* **2013**, *60*, 20–30. [[CrossRef](#)]
38. Kandasamy, V.; Manoj, R. Grid integration of AC and DC energy resources using multi-input nine switch matrix converter. In Proceedings of the 2014 International Conference on Green Computing Communication and Electrical Engineering (ICGCCEE), Coimbatore, India, 6–8 March 2014; pp. 1–4.